Science of the Total Environment 756 (2021) 144146

Contents lists available at ScienceDirect

Science of the Total Environment

journal homepage: www.elsevier.com/locate/scitotenv

Responses of bacterial communities and their carbon dynamics to subsoil exposure on the Loess Plateau

Qiqi Sun [a,b,c], Shengli Guo [a,b], Rui Wang [a,b,*], Jinming Song [c,**]

[a] State Key Laboratory of Soil Erosion and Dryland Farming on the Loess Plateau, Institute of Soil and Water Conservation, Northwest A&F University, Yangling, Shannxi 712100, PR China
[b] State Key Laboratory of Soil Erosion and Dryland Farming on the Loess Plateau, Institute of Soil and Water Conservation, Chinese Academy of Sciences and Ministry of Water Resources, Yangling, Shannxi 712100, PR China
[c] Key Laboratory of Marine Ecology and Environmental Sciences, Institute of Oceanology, Chinese Academy of Sciences, Qingdao, Shandong 266071, PR China

HIGHLIGHTS

- Subsoil exposure had depth-specific effect on bacterial community and activities.
- Both copiotrophic and oligotrophic groups increased in exposed vs. control soil.
- Bacterial community composition altered at 60–100 cm in exposed vs. control soil.
- Enzyme activities were greater at 20–60 and 60–100 cm in exposed vs. control soil.
- The exposed subsoils had consistently lower K_c and Q_{10} compared with the topsoil.

GRAPHICAL ABSTRACT

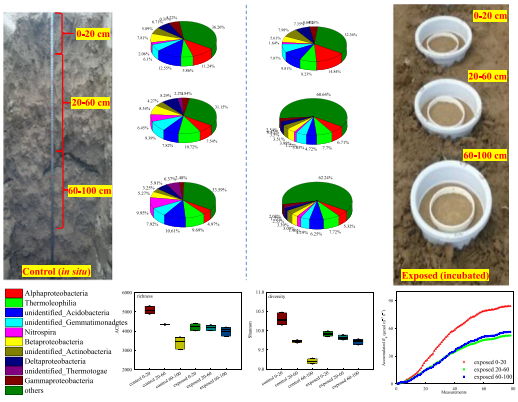

ARTICLE INFO

Article history:
Received 13 August 2020
Received in revised form 24 November 2020
Accepted 24 November 2020
Available online 28 November 2020

Editor: Yucheng Feng

Keywords:
Subsoil exposure
Bacterial community composition
Enzyme activity
Carbon mineralization rate
Temperature sensitivity

ABSTRACT

Subsoil exposure due to factors including erosion and terracing, evidently decreases soil organic carbon storage and productivity, but the responses of bacterial communities and their carbon dynamics remain unclear. Soils from 0–20 cm, 20–60 cm and 60–100 cm were collected from three 100 cm profiles in bare land on the Loess Plateau, and incubated in buried pots for a year (July 2016 to July 2017) to simulate subsoil exposure, with ongoing monitoring of the microbial mineralization rate of soil organic carbon (K_c), using Li-Cor 8100. At the end of the incubation period, the exposed soil and the in situ control soil were sampled to investigate changes in bacterial community composition, as represented by 16S rRNA, and the activities of enzymes involved in soil carbon cycling. Both copiotrophic (Actinobacteria and Alphaproteobacteria) and oligotrophic (Thermoleophilia) groups were stimulated in the exposed vs. control soil at 20–60 and 60–100 cm. The exposed vs. control soil from 60 to 100 cm produced the greatest bacterial responses, such as greater diversity and altered keystone groups (Thermoleophilia vs. unidentified Acidobacteria). Enzyme activities were greater in the exposed vs. control soil at both 20–60 cm (β-D-xylosidase and cellobiohydrolase) and 60–100 cm (β-D-xylosidase and β-D-glucosidase). The exposed soil from 20–60 cm and 60–100 cm had lower K_c and Q_{10} values than those at 0–20 cm. Our findings revealed the existence of bacterial depth-specific responses to subsoil exposure, and highlight the effect of anthropogenic soil redistribution on soil carbon flux and its potential responses to future climate change.

* Correspondence to: R. Wang, Institute of Soil and Water Conservation, Xinong Road No. 26, Yangling, Shaanxi 712100, PR China.
** Correspondence to: J. Song, Institute of Oceanology, Nanhai Road No. 7, Qingdao, Shandong 266071, PR China.
E-mail addresses: ruiwang0212@126.com (R. Wang), jmsong@qdio.ac.cn (J. Song).

https://doi.org/10.1016/j.scitotenv.2020.144146
0048-9697/

1. Introduction

Subsoil exposure via accelerated soil erosion and other anthropogenic soil redistribution such as tillage, terracing and land leveling, has now been recognized as a global problem (Berhe et al., 2007b; Brye et al., 2004; Eck, 1987). Soil erosion, which can cause substantial subsoil exposure (Lal, 2003), was estimated to redistribute as high as 30–100 Pg soil per year on a global scale (Berhe et al., 2007a; Stallard, 1998; Walling, 2009). Subsoil exposure inevitably affects the redistribution of soil organic carbon (SOC) in the surface and/or subsurface soil, as well as affecting regional and even global soil carbon cycling. Once exposed, SOC and its major biotic degradation driver, microorganisms, in the subsoil face divergent fates compared with those being buried. Therefore, it is essential to investigate the effect of subsoil exposure on microbial properties and their involved carbon cycling, to clarify the role of exposed subsoil in the soil carbon budget of severely eroded areas.

Soil bacteria, which contribute 70%–90% of soil microbial biomass (Bardgett et al., 2008), play a critical role in driving C cycling and maintaining C storage in terrestrial ecosystems (Azam and Malfatti, 2007; de Carvalho et al., 2016; Takriti et al., 2018). Bacterial diversity significantly decreases with soil depth (Li et al., 2019), and bacterial community composition changes vertically, with differences observed even within millimeters (Li et al., 2019; Yan et al., 2019b). Microbial trophic guilds, which may be coupled with potential carbon dynamics (Bai et al., 2017), are predicted to shift as they vary with soil layers. When topsoil is removed and the SOC therein is transported away, microbial biomass and diversity tend to decrease, due to lower available C and N substrate supplies (Sushko et al., 2019). Both variation in the abundance of important microbial species (Yan et al., 2019a) and alteration of keystone taxa (Gao et al., 2020) between exposed subsoil and soil in situ have been observed, and these differences are partially due to the reduced substrate supply and/or altered substrate quality. Specific microbial populations may switch from an anoxic to an oxic state, and grow actively when the subsoil is exposed to air (Yan et al., 2019a), potentially changing the microbial community composition. Tremendous microbial variation between exposed subsoil and control groups is predictable, as even subtle soil perturbations can provoke dramatic changes in microbes (Aylagas et al., 2016; Simonin et al., 2019). However, to our knowledge, few studies concerning the effect of subsoil exposure on microbes have been conducted into differences in in situ and exposed soils.

Soil redistribution included subsoil exposure is playing increasingly important role in the soil carbon cycling in response to global warming (Gao et al., 2020; Li et al., 2018), which introduces considerable uncertainty when estimating soil C budget at regional scale (Davidson et al., 2006). Numerous researches have demonstrated that upon being exposed to surface conditions, subsoils were generally characterized by lower SOC decomposition rate compared with the untreated topsoil (Bai et al., 2019; Gao et al., 2020), with the SOC stocks and microbial biomass carbon being deprived away. However, at present, no consensus has been achieved with regards to the temperature sensitivity of SOC decomposition (Q_{10}) in the exposed subsoil relative to the control topsoil. For instance, greater temperature sensitivities of soil CO_2 efflux in the exposed subsoils vs. untreated topsoil have been more observed in in situ topsoil removal experiment (Gao et al., 2020), in a short-term incubation experiment based on clay-loam loess (Bai et al., 2019), and in a study of paddy and cropland soils (Yan et al., 2017). In contrast, the results of previous study in alpine meadow sites (Qin et al., 2019) demonstrated that the SOC decomposition was more sensitive to warming in the incubated topsoil than in the incubated subsoil. In addition, neutral response of Q_{10} to depths-related changes in SOC components was also observed with the incubated soil (Fang et al., 2005). Therefore, how subsoil exposure from various depths affects the SOC decomposition rate as well as its response to temperature changes is of critical relevance to soil use and management, especially when confronting future climate change.

In the present study, an in situ soil pots incubation experiment simulating subsoil exposure was conducted on the Loess Plateau from July 2016 to July 2017. Our aims were to 1) investigate the response patterns of bare-soil bacterial communities and their enzyme activities to subsoil exposure at different soil depths; 2) identify the factors determining variation in bacterial communities and enzyme activities between the exposed soil and the in situ soil at different depths; and 3) estimate differences in SOC decomposition rate and temperature sensitivity at various depths in the exposed soil. We hypothesized that 1) bacterial communities in deeper subsoil would be less responsive to exposure due to the lower C and N content of the subsoil; and 2) the exposed subsoils would have lower K_c because of their less labile C and N contents but higher Q_{10} than the topsoil, due to the greater stability of their C and N substrates.

2. Materials and methods

2.1. Site description

A typical site of bare land (17.5 m × 5.5 m) was used for a case study at the Changwu State Key Agro-ecological Experimental Station (E107°40′, N35°12′), which is located on the southern Loess Plateau in the middle reaches of the Yellow River, northern China (Fig. 1, cited from Wang et al., 2017). The Loess Plateau is known for its long agricultural history, and has experienced serious soil erosion (Lal, 2003). The study area is characterized by a semiarid continental monsoon climate, with a mean annual temperature of 9.4 °C (1957–2015). Most of the mean annual rainfall occurs between July and September in the form of thunderstorms (Huang et al., 2003). Due to the joint effect of a thick soil layer and highly intensive rainfall, severe soil and water losses occurred under non-vegetated conditions, which can occasionally account for 50%–70% of the losses for the entire year. Therefore, bare soils suffer from frequent and serious subsoil exposure. To improve the natural landscape and increase productivity levels, large-scale farmland construction, such as tillage, terrace construction and land leveling, has been conducted in this region since the establishment of China. These activities, however, exposed a large area of infertile subsoil due to topsoil disturbance. In addition, increase in temperature has been predicted on the Loess Plateau due to climate change (Zhi et al., 2010), which will aggravate effects of subsoil exposure.

In the study site, soils within a 100 cm profile were stratified in the following order: 0–20 cm is the cultivated horizon, 20–60 cm is the ancient cultivated horizon and 60–100 cm is the black loessial soil horizon (Li and Su, 1991). The soil is a uniform loam (Cumulic Haplustoll; USDA Soil Taxonomy System) which originated from a parent material of calcareous loess. It contains 24% clay (<0.002 mm), 10.5% $CaCO_3$, 6.5 g kg^{-1} organic C, and 0.80 g kg^{-1} total nitrogen. The soil has a field water-holding capacity of 0.29 cm^3 cm^{-3}, a pH of 8.4 (1:1 soil: H_2O suspension), and a bulk density of 1.3 g cm^{-3} within a depth of 0–20 cm.

2.2. Soil pot experiment

The experiment included two treatments: 1) exposed soil, which was sampled from the in situ soil profile and incubated in soil pots for one year; 2) control soil, which was sampled from the in situ soil profile. The in situ soil was assumed to be stable and invariant compared with that one year ago under certain conditions of the Loess Plateau, which was considered to be a rational precondition following Li and Su (1991).

On bare land, three 100 cm soil profiles were established in June 2016, with the profiles located more than 2 m from each other. The soils used for the incubation experiment were collected at depths of 0–20, 20–60, and 60–100 cm, after surface litter and aboveground vegetation was removed. After the roots were removed, the samples collected from the same depth in each of the replicated profiles were individually mixed, air-dried and passed through a 2 cm sieve for

homogenization, yielding three samples for each depth. In the outdoor incubation, soil samples of 25 kg each were packed to a bulk density of 1.25 g cm^{-3}, the average of soil bulk density, in polyvinyl chloride pots, 32 cm in diameter and 25 cm in height, and maintained at field capacity water content throughout the incubation period. Each depth was sampled in triplicate, so that a total of nine pots were acquired. The pots were perforated to allow exchange of gases, heat, and water with the surroundings, and to prevent waterlogging.

The incubation experiment was conducted using in situ incubation of soil samples. At the experimental station near the sampling site, soil pots containing soil samples from the three depths were buried in a random combination (Fig. 1b). The pots were buried in soil with a rim of 2 cm, to prevent surface runoff from entering the pots. The rim was covered to avoid direct sunlight, and the direct surroundings were reestablished as before. After the establishment of the soil pots, a polyvinyl chloride collar, 20 cm in diameter and 6 cm in height, was inserted into the soil to a depth of 2 cm at the center of each pot, to measure the microbial SOC mineralization rate. All soil samples were incubated for the entire experimental period (July 2016 to October 2017) in the pots, with the top open to the atmosphere, under ambient air temperature conditions. The green parts of grasses within the collar as well as any new grasses growing during the incubation, were cut off. Water loss during the incubation period was periodically checked volumetrically and adjusted accordingly.

2.3. Measurement of microbial SOC mineralization rate

Measurements of the SOC decomposition rate were started after two weeks of stabilization, to allow soil samples to recover from sampling disturbance. During the incubation period, the microbial mineralization rates of SOC (K_c) were measured every three days to determine the response of the soil at different depths to soil temperature, by mounting a soil CO_2 flux system (a portable chamber 20 cm in diameter, Li-8100, Lincoln, NE, USA) onto the collars. All measurements were conducted between 9:00 am and 11:00 am (Iqbal et al., 2009). The K_c of each depth was calculated as the mean of the three collar measurements. For each collar, the average of two measurements was taken as the microbial mineralization rate to avoid outliers. When the variation between two measurements was less than 15%, the measurements were considered to be reliable. However, if the variation between two measurements was larger than 15%, one or more measurements were taken until the variation was less than 15%. Soil temperature (two replicates per collar) at a depth of 5 cm depth was measured at the same time as the K_c measurement, using a Li-Cor thermocouple probe 1 cm away from the collar.

2.4. Soil sampling and biochemical analysis

To measure the soil biochemical properties, nine soil samples—three soil cores from 0 to 20 cm, three soil cores from 20 to 60 cm, and three from 60 to 100 cm—were taken from the in situ soil as a control in July 2016, and from the exposed soil in the pots at the end of incubation in July 2017, using a soil auger 3 cm in diameter. Each sample, comprised of three subsamples randomly collected at each depth, was crushed through a 2.0 mm sieve immediately after sampling, and divided into three parts: one was stored at −80 °C for DNA extraction, the second was stored at 4 °C for less than four days to determine the enzyme activities, soil microbial biomass (SMBC), dissolved organic carbon (DOC), soil nitrate (NO_3-N), and ammonium (NH_4-N) nitrogen contents. The third part was air dried, crushed to pass through a 0.15 mm sieve, and used for the qualification of soil total organic carbon (SOC) and soil total nitrogen (TN).

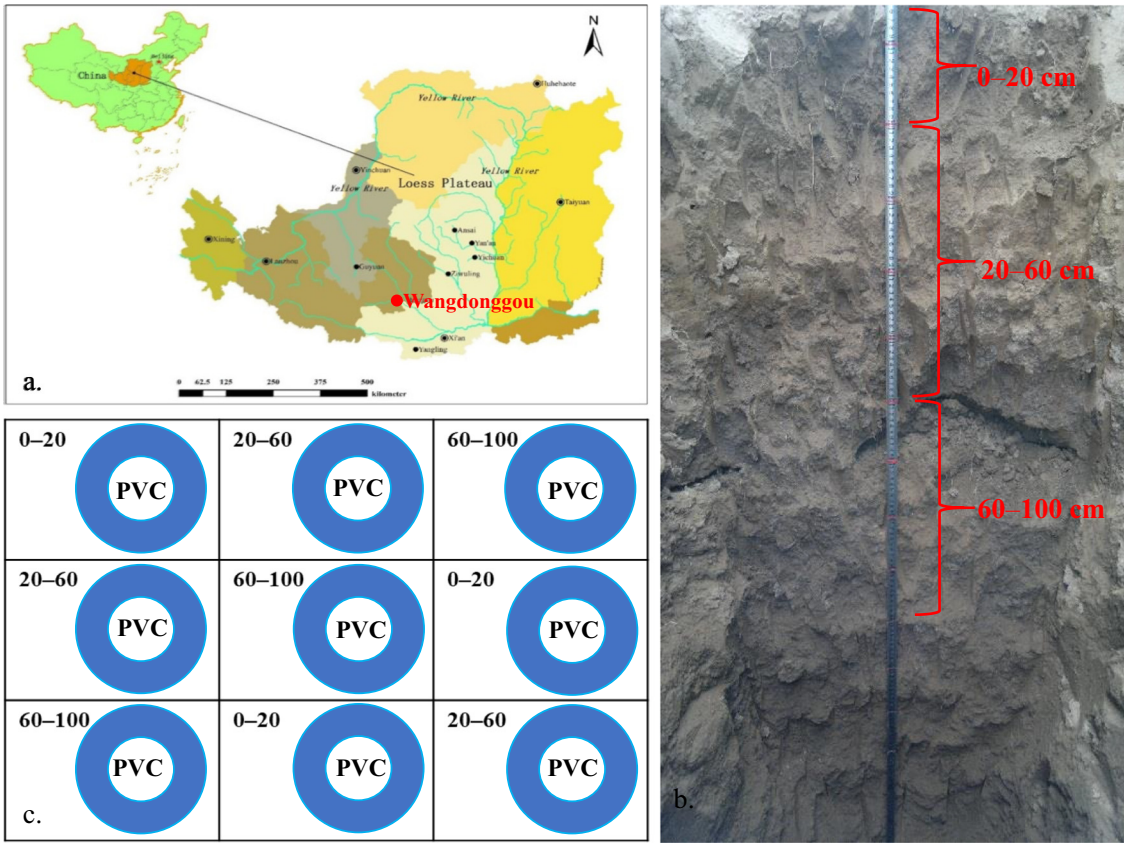

Fig. 1. Location of the experimental site in the Loess Plateau, China (a. cited from Wang et al., 2017), the in situ soil profile (b.) and the incubated experiment (c.)

SOC was measured using the K_2CrO_7-H_2SO_4 oxidation method (Sparks et al., 1996). TN was measured using the Kjeldahl method. The field-moist soil samples, equivalent to 15 g oven-dried soil, were extracted with 60 mL of 0.5 M K_2SO_4, and shaken for 60 min at 200 rpm on a reciprocal shaker. The DOC content was measured using a total organic carbon analyzer (TOC-VCSH, Shimadzu, Japan) (Fujii et al., 2011; Vance et al., 1987). The soil nitrate nitrogen (NO_3-N) and ammonium nitrogen (NH_4-N) were extracted with 2 M KCl at a 1:5 ratio, filtered, and then measured using colorimetry at 625 nm and 220 nm, with a Bran & Luebbe II AutoAnalyzer (Fernández-Escobar et al., 2009). The SMBC content was determined using the chloroform fumigation-extraction method, with a scale factor of 0.45 (Vance et al., 1987). In this study, fluorometric substrates linked to 4-MUB-β-D-xyloside, 4-MUB-β-D-glucoside and 4-MUB-cellobioside from Sigma (St Louis, MO, USA) were used for assays of the three extracellular C-acquiring enzymes: β-D-xylosidase (BX), releases xylose from hemicellulose (Kirschbaum, 2013); β-D-glucosidase (BG), representing the enzyme associated with the breakdown of recalcitrant C (Du et al., 2010); and cellobiohydrolase (CB), releases disaccharides from cellulose (Kirschbaum, 2013) (Deforest, 2009). All substrates were purchased from Sigma-Aldrich (St. Louis, MO, USA). Activities were expressed as nanomoles of substrate released per hour per gram of SOC (nmol g^{-1} h^{-1}).

2.5. DNA extraction and Illumina HiSeq high-throughput sequencing

Total genomic DNA from each sample was extracted from 0.5 g soil using the CTAB/SDS method with Qiagen Gel Extraction Kits (Qiagen, Germany). The 515F and 806R primers were designed to amplify the hypervariable V3–V4 region of the 16S rRNA gene from the bacteria (Caporaso and Gordon, 2011). For sequencing, PCR products were mixed in equidense ratios. The PCR products were purified with Qiagen Gel Extraction Kits (Qiagen, Germany). TruSeq® DNA PCR-Free Sample Preparation Kits (Illumina, USA) were used to generate sequencing libraries, and the Qubit® 2.0 Fluorometer (Thermo Scientific) and Agilent Bioanalyzer 2100 system were used to assess the library quality. Sequencing was conducted on an Illumina HiSeq 2500 platform (Illumina Corporation, San Diego, CA, USA).

Sequence analysis and operational taxonomic unit (OTU) clustering were performed using the UPARSE software package with the UPARSE-OTU and UPARSE-OTU ref algorithms (Edgar, 2013). The taxonomy of the specimens was established using the Ribosomal Database Project classifier (Wang et al., 2007). Relative abundance was calculated as the number of OTUs affiliated with the same phylogenetic group divided by the total number of OTUs. Each sample was rarefied to produce the same number of reads (80,208 sequences) for both alpha-diversity and beta-diversity analyses, with an average length of 253 bp. Alpha-diversity indices including the Chao1 estimator of richness, Abundance-based Coverage Estimator (ACE), Shannon diversity index, and Simpson diversity index were generated based on the obtained OTUs. The ACE and Shannon diversity indices were used to estimate the species richness and diversity of the bacterial communities. The high-throughput sequencing data were uploaded to the NCBI Sequence Read Archive database with accession numbers SUB3054666 and SUB3100896.

2.6. Statistical analysis

The relationship between the soil microbial SOC mineralization rate and soil temperature was established by fitting an exponential function (Davidson et al., 1998):

$$y = \beta_0 e^{\beta 1 T} \quad (1)$$

where y is the measured microbial SOC mineralization rate (K_c, μmol m^{-2} s^{-1}), and T is the measured soil temperature (°C) at a specific depth.

The temperature sensitivity of the microbial C mineralization rate (Q_{10}) was calculated as previously reported (Xu and Qi, 2001):

$$Q_{10} = e^{10\beta 1} \quad (2)$$

A t-test of independent samples was conducted to assess the effect of exposure on alpha-diversity indices, soil bacterial communities and biochemical properties between the two soils. The results are reported as mean ± SD ($n = 3$), $P < 0.05$ was taken as indicating statistical significance. One-way analysis of variation (ANOVA) and least significant difference (LSD) multiple comparisons ($P < 0.05$) were performed to assess differences in microbial properties, soil parameters, K_c, and Q_{10} among the depths of the exposed soil (mean ± SD, $n = 3$). Principal Coordinate Analysis (PCoA) was used to identify dissimilarities in the bacterial community structure. Pearson correlation analysis and redundancy analysis (RDA) were used to identify the most important environmental variables influencing bacterial groups. SPSS 20.0 software (SPSS Inc., Chicago, USA) was used to conduct statistical analyses, and SigmaPlot 12.5 software (Systat Software Inc., San Jose, CA, USA) was used to generate figures. PCoA and RDA were performed using R software package v.3.6.1 (Team, 2013).

3. Results

3.1. Differences between soil variables in exposed vs. control soil

The SOC, TN, and soil C/N ratio varied little, while the available C and N differed between the exposed and the control soil (Table 1). DOC was slightly higher at depths of 0–20 cm and 20–60 cm, but at 60–100 cm was significantly greater in the exposed soil than in the control soil, by 7.3 times ($P < 0.05$). The soil mineral N, made up of the sum of NO_3-N and NH_4-N, was 104.3% greater in the exposed vs. control soil at depths of 20–60 cm ($P < 0.05$) and 51.1% greater in exposed soil at 60–100 cm ($P < 0.05$). The exposed subsoil had slightly but non-significantly higher SMBC than the control soil at 20–60 cm (by 23.4%) and 60–100 cm (by 194.9%). However, the enzyme activities had varying and significant differences (Table 1). At 20–60 cm, the activities of BX and CB in the exposed soil were 122.0% ($P < 0.05$) and 360.5% ($P < 0.05$) greater than in the control soil. At 60–100 cm, the BX and BG activities were 112.0% ($P < 0.05$) and 194.4% ($P < 0.05$) greater, while CB activity was 65.4% ($P < 0.05$) lower, in the exposed soil than in the control soil.

3.2. Changes in bacterial properties in the exposed vs. control soils

For both soils, the number of unique OTUs, a metric which is indicative of the complexity of the ecosystem, were greatest at 0–20 cm, followed by 20–60 cm, and then 60–100 cm (Fig. 2a), with the range of variation smaller in the exposed soil than in the control soil. ACE richness and Shannon diversity indices in both soils decreased with depth, with a smaller range of variation in the exposed vs. control soil (Fig. 2b). Greater diversity in the exposed vs. control soil was only observed at 60–100 cm ($P < 0.05$, Table 2). The rarefaction curves of all soil samples tended to be gentle (Fig. 3a), with coverage reaching up to over 95%. PCoA identified dissimilarity in the bacterial community structure between the exposed and control soils, with the distances increasing with depth (Figs. 3b, S1).

Proteobacteria, Actinobacteria, Acidobacteria and Gemmatimonadetes were predominant in the bacterial communities across all samples, representing the majority of the bacterial reads in the control (68.0%) and exposed soil (74.4%) (Table 3, Fig. 4). At the phylum level, soil bacterial community composition changed from being Proteobacteria-dominated at 0–20 cm and 20–60 cm, to Actinobacteria-dominated at 60–100 cm, for both soils (Fig. 4a and b). The exposed soil from 20–60 and 60–100 cm consistently had increased abundance of Proteobacteria, Actinobacteria, and Bacteroidetes, and decreased abundance of Nitrospirae, Thermotogae, and Chloroflexi.

Table 1
Soil properties in the control and the exposed soils at 0–20, 20–60 and 60–100 cm.

Items	0–20 cm		20–60 cm		60–100 cm	
	Control	Exposed	Control	Exposed	Control	Exposed
T/°C	23.0 ± 0.8a	25.0 ± 1.4a	21.6 ± 0.7a	24.9 ± 1.4a	19.3 ± 0.6a	25.0 ± 1.4b
SOC/g kg^{-1}	8.44 ± 0.19a	8.44 ± 0.19a	5.48 ± 0.19a	5.48 ± 0.19a	7.52 ± 1.09a	7.52 ± 1.09a
TN/g kg^{-1}	0.73 ± 0.06a	0.73 ± 0.06a	0.33 ± 0.02a	0.33 ± 0.02a	0.37 ± 0.00a	0.37 ± 0.00a
C/N	11.82 ± 1.20a	11.82 ± 1.20a	16.61 ± 0.44a	16.61 ± 0.44a	20.37 ± 2.97a	20.37 ± 2.97a
DOC/mg kg^{-1}	52.62 ± 4.78a	63.18 ± 7.97a	19.08 ± 4.46a	25.20 ± 3.53a	4.31 ± 1.92a	31.64 ± 4.23b
N_{min}/mg kg^{-1}	40.37 ± 6.81a	55.22 ± 1.56a	22.70 ± 2.94a	46.37 ± 2.06b	18.58 ± 2.52a	28.07 ± 2.35b
SMBC/mg kg^{-1}	125.44 ± 11.98a	123.25 ± 17.88a	45.92 ± 7.89a	56.67 ± 5.92a	12.50 ± 1.71a	36.86 ± 11.44a
BX/nmol g^{-1} h^{-1}	15.05 ± 0.68a	17.10 ± 2.33a	1.73 ± 0.08a	3.84 ± 0.75b	0.83 ± 0.28a	1.76 ± 0.07b
BG/nmol g^{-1} h^{-1}	34.75 ± 5.75a	29.93 ± 5.18a	6.11 ± 0.35a	11.62 ± 2.31a	1.96 ± 0.22a	5.77 ± 0.67b
CB/nmol g^{-1} h^{-1}	7.51 ± 2.25a	9.72 ± 2.15a	0.38 ± 0.13a	1.75 ± 0.15b	1.90 ± 0.16b	0.66 ± 0.23a

Note: T is short for soil temperature at the sampling time. SOC is the total soil organic carbon; DOC is soil dissolved organic carbon. TN is the total nitrogen content; N_{min} is the soil mineral nitrogen content. C/N is the soil C:N ratio. SMBC is soil microbial biomass carbon. BX is short for β-D-xylosidase, BG is β-D-glucosidase and CB is cellobiohydrolase. Different letters in a column indicate significant difference between the control and the exposed soil at $P < 0.05$, values are means of three replicates ± SE ($n = 3$).

However, the magnitude of increases at 60–100 cm was greater than that at 20–60 cm. Proteobacteria was increased by 21.0% at 60–100 cm vs. 3.1% at 20–60 cm, and Actinobacteria was increased by 23.8% at 60–100 cm vs. 18.3% at 20–60 cm (Table 3). At the class level, the soil bacterial community composition was dominated by Thermoleophilia for both soils at 20–60 cm, while bacterial community composition changed from unidentified_Acidobacteria-dominant in the control soil to Thermoleophilia-dominant at 60–100 cm in the exposed soil (Fig. 4c and d). At 20–60 cm, the Alphaproteobacteria, Thermoleophilia, and unidentified_Actinobacteria were 54.2%, 24.3%, and 42.4% more abundant in the exposed vs. control soil, while Nitrospira, Deltaproteobacteria, and unidentified_Thermotogae were 3 times, 1.4 times, and 2.9 times less abundant, respectively, in the exposed vs. control soil (Table 3). The same pattern was also observed at 60–100 cm, of greater magnitude than at 20–60 cm. The exposed soil at 60–100 cm also had increased abundance of Gammaproteobacteria (by 45.3%) than the control soil (Table 3).

Taking into account the correlation results (Tables S1–S3), the soil variables DOC, SMBC, and soil mineral N were selected to conduct RDA. Soil mineral N influenced the variation in the 16S rRNA of bacteria between the exposed soil and the control soil at 0–20 cm ($r^2 = 0.87$, $P < 0.1$) (Fig. 5a). At 20–60 cm, 94.1% of the total variation was explained by these variables ($P < 0.05$) (Fig. 5b), and soil mineral N was the factor that most significantly influenced the variation in the 16S rRNA of bacteria between the two soils ($r^2 = 0.97$, $P < 0.05$). At 60–100 cm, these variables explained 86.5% of the total variation

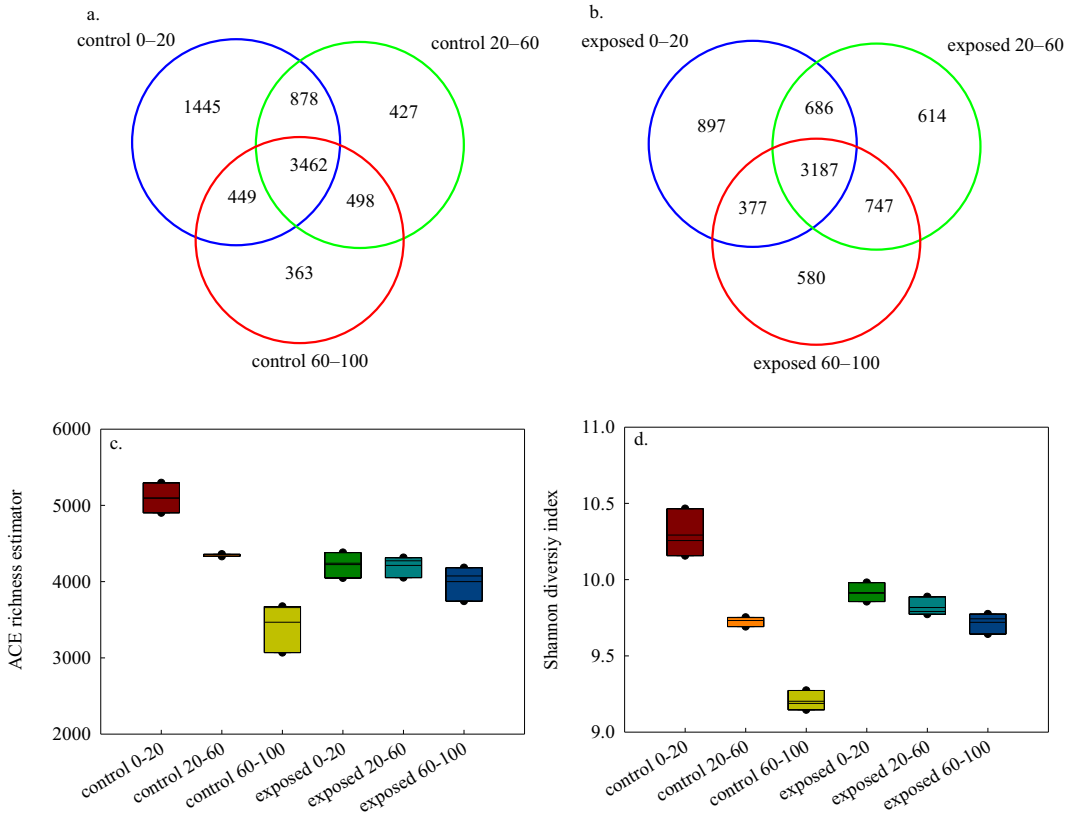

Fig. 2. Unique OTUs for the bacteria from the samples at each depth of the exposed (a.) and the control (b.) soils and boxplots of alpha diversity indices (c. ACE richness and d. Shannon diversity indices) of the exposed and control soils.

Table 2
Alpha diversity at depth of 77,801 sequences in the control and 76,311 sequences in the exposed soil per sample of bacterial community.

Depths/cm	Treats	Chao1	ACE	Shannon	Simpson
0–20	Control	4884 ± 28b	5097 ± 93b	10.193 ± 0.09b	0.998 ± 0.000a
	Exposed	4146 ± 86a	4323 ± 87a	9.915 ± 0.04a	0.997 ± 0.00a
20–60	Control	4258 ± 62a	4398 ± 98a	9.732 ± 0.02a	0.997 ± 0.00a
	Exposed	4145 ± 93a	4213 ± 81a	9.817 ± 0.04a	0.997 ± 0.00a
60–100	Control	4086 ± 501a	4134 ± 468a	9.002 ± 0.04a	0.995 ± 0.00a
	Exposed	3955 ± 152a	4000 ± 132a	9.720 ± 0.04b	0.997 ± 0.00b

Note: Chao1 is short for Chao1 estimator of richness, ACE is short for ACE estimator of richness, Shannon is short for the Shannon diversity index and Simpson is short for the Simpson diversity index. Different letters in a column indicate significant difference between the control and the exposed soils at $P < 0.05$, values are means of three replicates ± SE ($n = 3$).

($P < 0.01$) (Fig. 5c), with soil mineral N ($r^2 = 0.85$, $P < 0.05$) and DOC ($r^2 = 0.88$, $P < 0.1$) being the environmental gradients influencing the variation in the 16S rRNA of bacteria between the two soils. In the exposed soil, SOC, TN, C/N, DOC, and soil mineral N explained 91.8% of the total variation among depths, with DOC ($r^2 = 0.88$, $P < 0.01$), soil mineral N ($r^2 = 0.87$, $P < 0.05$), and TN ($r^2 = 0.82$, $P < 0.05$) being the environmental gradients with the most influence on variation in the 16S rRNA of bacteria (Table S4, Fig. 5d).

3.3. K_c and Q_{10} were lower in the exposed subsurface than in the topsoil

In the exposed soil, the mean K_c at 20–60 cm (0.67 ± 0.05 μmol m^{-2} s^{-1}) and 60–100 cm (0.72 ± 0.04 μmol m^{-2} s^{-1}) were 61.6% ($P < 0.05$) and 51.4% ($P < 0.05$) lower than that at 0–20 cm (1.09 ± 0.04 μmol m^{-2} s^{-1}), with no significant difference between 20–60 cm and 60–100 cm (Fig. 6a, $P > 0.05$). Similarly, the Q_{10} were 27.7% ($P < 0.05$) and 31.5% ($P < 0.05$) lower at 20–60 cm (2.37 ± 0.16) and 60–100 cm (2.30 ± 0.12) than at 0–20 cm (3.03 ± 0.40), with no significant difference between 20–60 cm and 60–100 cm (Fig. 6b, $P > 0.05$). Both K_c and Q_{10} had significant positive correlations with TN, abundance of Alphaproteobacteria (genus *Microvirga*), and unidentified Actinobacteria (genus *Blastococcus*) (Table S4). Additionally, K_c was positively correlated with SMBC, enzyme activities, and abundance of Deltaproteobacteria (genus *Haliangium*), and negatively correlated with the abundance of Thermoleophilia (genus *Gaiella*) (Table S5). Q_{10} was positively correlated with SMBC and BX activities, and negatively correlated with NO_3-N.

4. Discussion

4.1. The greatest environmental changes were observed at 60–100 cm

Due to subsoil exposure, previously buried soils were exposed to various changes in environmental conditions, including exposure to air (especially O_2 and CO_2), higher soil temperatures, altered C input regimes, and microbial C accessibility (Table 1). Soil aeration and temperature generally decreased with depth (Weige et al., 2016), but was improved and tended to be equalized once exposed to the surface (Table 1). The C inputs of the subsoils in situ consisted mainly of plant residues and root exudate, and dissolved organic matter leaching from the overlying column, all of which also decreased with depth (Wang et al., 2019). A large amount of undecomposed bulk soil is maintained in the subsoils, especially at 60–100 cm, which provides better physical-mineral protection to the SOC from decomposition (Qin et al., 2019). However, subsoil exposure leads to the disruption of the bulk soil, breakdown of structural aggregates and exposure of hitherto encapsulated SOC and microorganisms to the ambient soil (Marin-Spiotta et al., 2014), resulting in an environment more suitable for the inhabiting microbes. Specially, at 20–60 cm, the disruption of the bulk soil and breakdown of soil aggregates led to increases in NO_3-N by 104.3% and DOC by 43.1% (Table 1). At 60–100 cm, the DOC and NO_3-N were highly stimulated from the oligotrophic niche, by 7 times for DOC and 1.5 times for NO_3-N (Table 1). Therefore, in the exposed subsoils, the main C inputs came from the disruption of native soil organic matter, which could release labile substrates and was controlled by N. The exposed soil from 60 to 100 cm is subject to the greatest

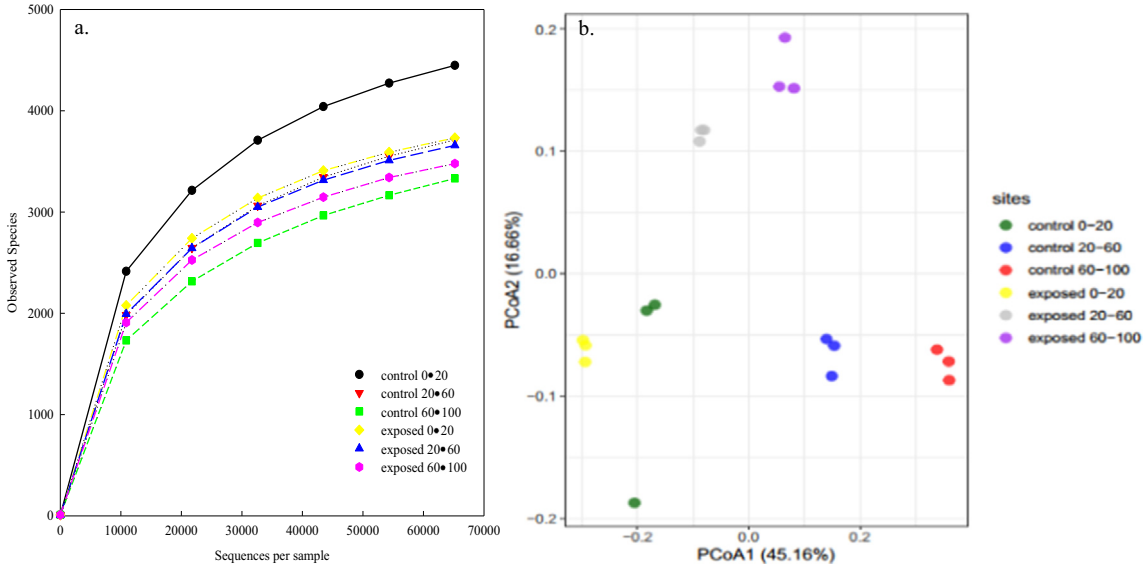

Fig. 3. Rarefaction curve (a.) based on the observed species of the two soils and principal Coordinate analysis (b. PCoA) of soil bacterial communities at three layers for the control (control 0–20, control 20–60, control 60–100) and the exposed (exposed 0–20, exposed 20–60, exposed 60–100) soils at the study site.

Table 3
Differences in the most abundant bacterial OTUs between the control and the exposed soils at 0–20, 20–60 and 60–100 cm depths.

Bacterial OTUs	0–20 cm		20–60 cm		60–100 cm	
	Control	Exposed	Control	Exposed	Control	Exposed
Phylum						
Proteobacteria	31.42 ± 1.97a	32.14 ± 2.52a	28.39 ± 0.19a	29.28 ± 0.14b	18.83 ± 0.38a	22.79 ± 0.81b
Actinobacteria	16.41 ± 2.44a	23.01 ± 1.66a	22.69 ± 0.91a	26.85 ± 0.52b	23.20 ± 0.98a	28.71 ± 1.48b
Acidobacteria	15.29 ± 0.67a	13.06 ± 1.34a	11.11 ± 0.31a	10.37 ± 0.29a	13.24 ± 0.43a	12.86 ± 0.18a
Gemmatimonadetes	6.10 ± 0.45a	7.87 ± 0.42b	9.39 ± 0.79a	8.74 ± 0.46a	7.92 ± 0.08a	7.25 ± 0.42a
Nitrospirae	2.06 ± 0.17a	1.64 ± 0.17a	6.45 ± 0.56b	2.12 ± 0.23a	9.95 ± 0.37b	3.40 ± 0.23a
Thermotogae	0.31 ± 0.10a	0.04 ± 0.01a	2.20 ± 0.18b	0.75 ± 0.04a	6.37 ± 0.63b	2.12 ± 0.34a
Firmicutes	4.83 ± 1.42a	2.74 ± 0.33a	4.43 ± 0.43a	5.07 ± 0.36a	3.53 ± 0.33a	4.32 ± 0.65a
Thaumarchaeota	1.69 ± 0.21a	2.85 ± 1.55a	2.03 ± 0.60a	2.52 ± 0.78a	2.11 ± 0.08a	1.64 ± 0.24a
Bacteroidetes	5.40 ± 0.28b	4.21 ± 0.20a	1.86 ± 0.13a	3.59 ± 0.23b	1.66 ± 0.14a	3.93 ± 0.29b
Chloroflexi	3.86 ± 0.57a	3.80 ± 0.41a	4.13 ± 0.09b	2.77 ± 0.11a	4.63 ± 0.13b	3.09 ± 0.07a
Class						
Alphaproteobacteria	11.20 ± 0.40a	14.82 ± 1.20b	7.55 ± 0.10a	11.63 ± 0.22b	4.97 ± 0.11a	9.21 ± 0.32b
Thermoleophilia	5.91 ± 0.60a	8.21 ± 2.00a	10.76 ± 0.10a	13.33 ± 0.32b	9.69 ± 0.32a	13.37 ± 0.64b
unidentified_Acidobacteria	12.61 ± 0.80b	9.85 ± 1.50a	7.82 ± 0.30a	8.18 ± 0.32a	10.61 ± 0.43a	10.82 ± 0.15a
unidentified_Gemmatimonadetes	6.14 ± 0.50a	7.91 ± 0.40a	9.36 ± 0.80a	8.74 ± 0.52a	7.92 ± 0.14a	7.25 ± 0.46a
Nitrospira	2.11 ± 0.20a	1.67 ± 0.20a	6.45 ± 0.60b	2.12 ± 0.22a	9.95 ± 0.44b	3.40 ± 0.23a
Betaproteobacteria	7.85 ± 1.00a	5.68 ± 0.60a	8.34 ± 0.50a	6.89 ± 0.42a	5.27 ± 0.13a	5.35 ± 0.42a
unidentified_Actinobacteria	5.93 ± 1.10a	8.09 ± 0.60a	4.27 ± 0.30a	6.08 ± 0.13b	3.25 ± 0.33a	5.87 ± 0.64b
Deltaproteobacteria	6.77 ± 0.70a	7.43 ± 0.40a	8.29 ± 0.10b	6.06 ± 0.16a	5.91 ± 0.15b	4.41 ± 0.22a
unidentified_Thermotogae	0.36 ± 0.10a	0.05 ± 0.00a	2.20 ± 0.20b	0.75 ± 0.06a	6.37 ± 0.63b	2.48 ± 0.32a
Gammaproteobacteria	5.22 ± 0.44a	4.33 ± 0.35a	3.84 ± 0.15a	4.40 ± 0.27a	2.12 ± 0.28b	3.60 ± 0.30a
Order						
Nitrospirales	2.06 ± 0.17a	1.64 ± 0.17a	6.45 ± 0.56b	2.12 ± 0.23a	9.95 ± 0.37b	3.40 ± 0.23a
Gaiellales	2.92 ± 0.37a	3.35 ± 0.97a	6.75 ± 0.14a	7.91 ± 0.20b	7.14 ± 0.22a	9.01 ± 0.44b
Gemmatimonadales	4.28 ± 0.29a	6.04 ± 0.28b	8.14 ± 0.67a	7.59 ± 0.40a	7.31 ± 0.08a	6.56 ± 0.43a
Subgroup_6	7.25 ± 0.66a	5.05 ± 0.75a	4.22 ± 0.27a	4.19 ± 0.13a	6.68 ± 0.41a	6.41 ± 0.16a
Thermotogales	0.31 ± 0.10a	0.04 ± 0.01a	2.20 ± 0.18b	0.75 ± 0.04a	6.37 ± 0.63b	2.12 ± 0.34a
Sphingomonadales	4.39 ± 0.27a	5.27 ± 0.46a	2.14 ± 0.10a	4.88 ± 0.26b	1.30 ± 0.08a	4.03 ± 0.14b
Solirubrobacterales	2.93 ± 0.24a	4.86 ± 1.01a	3.96 ± 0.04a	5.40 ± 0.08b	2.54 ± 0.14a	4.35 ± 0.17b
Rhizobiales	3.15 ± 0.22a	4.69 ± 0.34b	2.55 ± 0.10a	3.31 ± 0.02b	1.64 ± 0.03a	2.55 ± 0.05b
Myxococcales	3.64 ± 0.61a	3.46 ± 0.16a	2.73 ± 0.16a	2.45 ± 0.19a	1.50 ± 0.02a	1.62 ± 0.02a
Rhodospirillales	2.84 ± 0.24a	4.17 ± 0.48a	2.38 ± 0.10a	2.82 ± 0.10b	1.66 ± 0.06a	2.12 ± 0.15b
Family						
Gemmatimonadaceae	4.28 ± 0.29a	6.04 ± 0.28b	8.14 ± 0.67a	7.59 ± 0.40b	7.31 ± 0.08a	6.56 ± 0.43a
0319-6A21	1.37 ± 0.14a	1.17 ± 0.11a	4.37 ± 0.58b	1.44 ± 0.22a	6.93 ± 0.26b	2.34 ± 0.17a
Thermotogaceae	0.31 ± 0.10a	0.04 ± 0.01a	2.20 ± 0.18b	0.75 ± 0.04a	6.37 ± 0.63b	2.12 ± 0.34a
Nitrosomonadaceae	3.28 ± 0.51a	2.24 ± 0.24a	4.03 ± 0.37b	2.14 ± 0.19a	2.69 ± 0.10b	1.87 ± 0.11a
Gaiellaceae	1.28 ± 0.14a	1.78 ± 0.41a	2.94 ± 0.10a	3.51 ± 0.13b	2.77 ± 0.11a	3.48 ± 0.19b
RB41	2.15 ± 0.18a	2.35 ± 0.56a	1.01 ± 0.11a	1.90 ± 0.22b	1.05 ± 0.04a	2.20 ± 0.06b
Veillonellaceae	1.89 ± 0.72a	0.00 ± 0.00a	0.69 ± 0.13a	0.65 ± 0.11a	0.90 ± 0.11a	0.97 ± 0.19a
Sphingomonadaceae	2.83 ± 0.20a	2.80 ± 0.20a	1.35 ± 0.07a	2.98 ± 0.18b	0.84 ± 0.05a	2.54 ± 0.05b
Comamonadaceae	1.82 ± 0.52a	0.81 ± 0.09a	0.97 ± 0.07a	1.01 ± 0.07a	0.95 ± 0.10a	1.18 ± 0.15a
Nitrospiraceae	0.68 ± 0.04a	0.46 ± 0.09a	1.81 ± 0.17b	0.67 ± 0.05a	2.31 ± 0.15b	0.83 ± 0.06a
Genus						
GAL15	0.31 ± 0.10b	0.04 ± 0.01a	2.20 ± 0.18b	0.75 ± 0.04a	6.37 ± 0.63b	2.12 ± 0.34a
Gaiella	1.28 ± 0.14a	1.78 ± 0.41a	2.94 ± 0.10a	3.51 ± 0.13b	2.77 ± 0.11a	3.48 ± 0.19b
Sphingomonas	2.51 ± 0.19a	2.61 ± 0.22a	1.21 ± 0.07a	2.79 ± 0.16b	0.73 ± 0.05a	2.36 ± 0.06b
Blastococcus	0.84 ± 0.11a	1.74 ± 0.14b	0.48 ± 0.06a	0.70 ± 0.03b	0.18 ± 0.01a	0.37 ± 0.02b
unidentified_Nitrospiraceae	0.40 ± 0.04a	0.28 ± 0.05a	1.18 ± 0.11b	0.37 ± 0.02a	1.64 ± 0.11b	0.42 ± 0.05a
Solirubrobacter	0.79 ± 0.05a	1.19 ± 0.29a	0.99 ± 0.03a	1.08 ± 0.03a	0.54 ± 0.02a	0.73 ± 0.03b
Haliangium	1.09 ± 0.20a	0.92 ± 0.04a	1.01 ± 0.09b	0.63 ± 0.08a	0.56 ± 0.01b	0.37 ± 0.01a
Lautropia	0.09 ± 0.04a	0.00 ± 0.00a	1.06 ± 0.27a	1.09 ± 0.26a	0.12 ± 0.04a	0.14 ± 0.05a
Microvirga	0.67 ± 0.12a	1.19 ± 0.10b	0.33 ± 0.04a	0.68 ± 0.03b	0.15 ± 0.01a	0.45 ± 0.02b
Streptococcus	0.24 ± 0.05b	0.00 ± 0.00a	0.93 ± 0.20a	0.89 ± 0.23a	0.28 ± 0.04a	0.30 ± 0.05a

Note: different letters in a row indicate significant difference between the control and the exposed soils at $P < 0.05$, values are means of three replicates ± SE ($n = 3$).

environmental changes, as the priming effect was greatest where there was the strongest environmental pressure (Chen et al., 2014). This effect was indicated by a greater increase in temperature (29.3% vs. 15.2%) and larger amount of DOC (7.3 vs. 1.3 times) and SMBC (2.9 vs. 1.2 times) released from soil, as compared with conditions at 20–60 cm (Table 1).

4.2. Bacterial depth-dependent responses to subsoil exposure

Our data identified a greater sensitivity of bacterial properties to subsoil exposure with increasing depth, especially at 60–100 cm (Tables 2, 3; Figs. 2–4), a phenomenon which could be related to the initial substrate availability at different soil depths. The greater quantity (DOC and N_{min} contents) and higher quality (lower C/N) of C and N substrates (Table 1) made soils at 0–20 cm and the 20–60 cm capable of supporting more diverse bacterial communities (Table 2, Fig. 2), which had stronger resistance to disturbance (Jousset et al., 2011). In contrast, the exposed subsoil from 60 to 100 cm with the lowest substrate availability (Table 1), was subject to the most significant increases in DOC and NO_3-N (Tables 1, S3), a situation which was assumed to be responsible for these soils having the greatest bacterial responses in terms of diversity (Table 2), community structure (Fig. 3b), and community composition (Table 3).

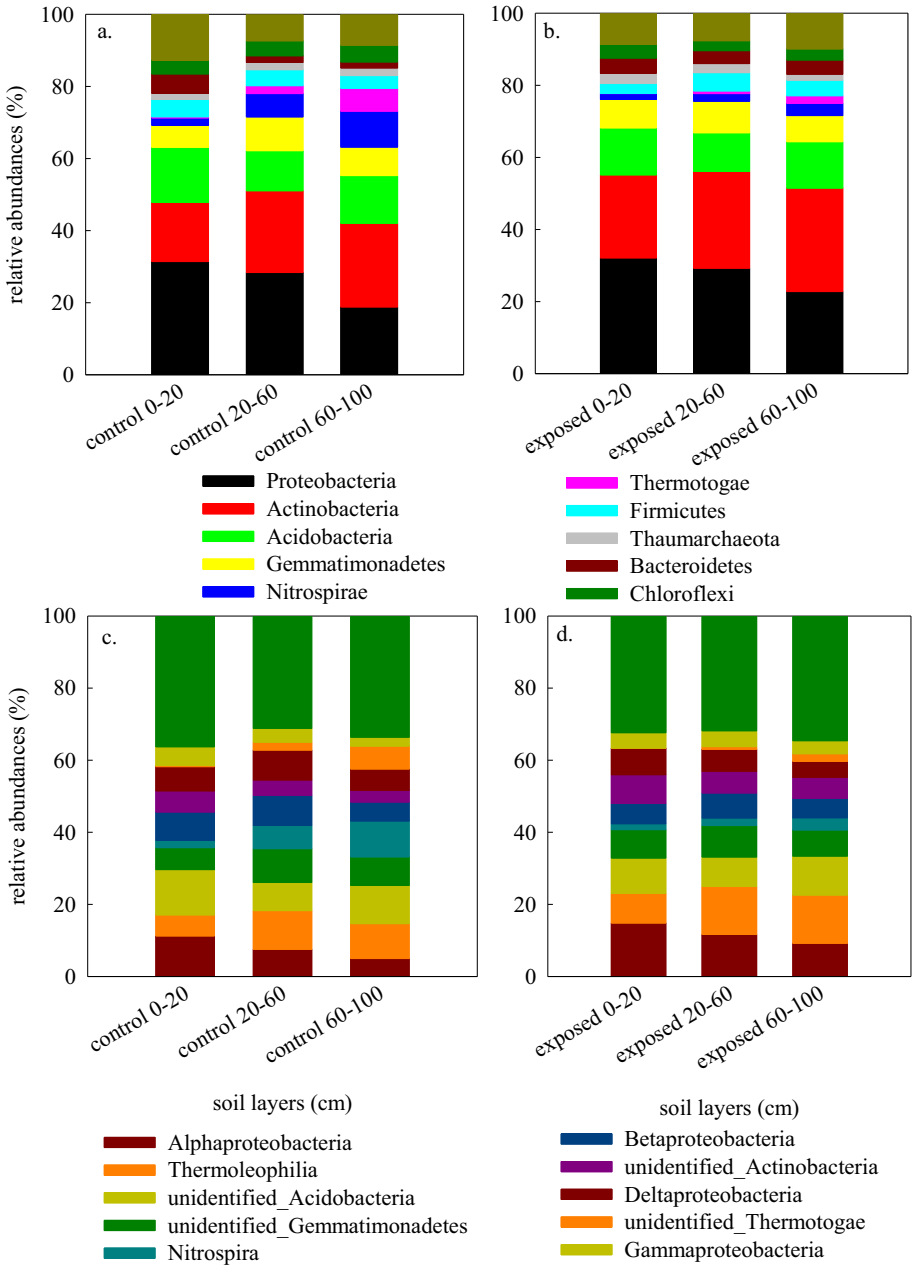

Fig. 4. Relative abundances of the dominant bacterial OTUs in different soil layers (0–20 cm, 20–60 cm and 60–100 cm) of the control and the exposed soils at the phylum (a. and b.) and the class (c. and d.) levels.

In this study, subsoil exposure affected bacterial communities, including the varied abundances of important species at 20–60 cm, and changes in predominant populations at 60–100 cm (Table 3, Fig. 4). NO_3-N (and DOC) significantly impacted bacterial communities in the N-limited exposed subsoils, leading to more abundant *r*-strategists and less abundant *K*-strategists than the control soil (Tables 3, S1, S2; Fig. 5) (Fierer et al., 2008). However, the oligotrophic Thermoleophilia (Table S4) was also stimulated probably due to their contribution to microbial N mining in terms of N limitation (Chen et al., 2014), as the subgroups were responsible for the decomposition of soil-derived organic matter such as aromatic compounds and polyphenols (Hu et al., 2019; Shi et al., 2020). Specific microbial populations respond to dramatic changes in microbial habitats, such as the change from anoxic to oxic conditions, causing decrease in the anaerobic and thermophilic Thermotogae (Frock et al., 2010). Sometimes, changes in microbial habitats overwhelmed the effects of changes in substrate, causing a decrease in the copiotrophic but anaerobic Deltaproteobacteria (order Myxococcales) (Treude et al., 2003). This situation was illustrated by FAPROTAX functional annotation (Louca et al., 2016), which predicted more abundant OTUs indicating aerobic metabolic pathways in the exposed soil than in the control soil (Fig. S2). At 60–100 cm, the oligotrophic niche was assumed to be responsible for the unidentified_Acidobacteria domination of the control soil. The highly stimulated DOC and NO_3-N (Table 1) further stimulated the number of *r*-strategists, leading to greater increases than at 20–60 cm, and depressed some of the *K*-strategists (Table S3). However, bacterial communities in the corresponding exposed soil were dominated by the oligotrophic Thermoleophilia (Table S4). This observation indicated the increased mineralization of native organic matter, which overwhelmed the effect of stimulated labile C and N substrates. This observation was reinforced by FAPROTAX functional annotation, which predicted more abundant OTUs indicating aromatic compound degradation and chitinolysis in the exposed soil than in the control soil (Fig. S2). Our results showed that

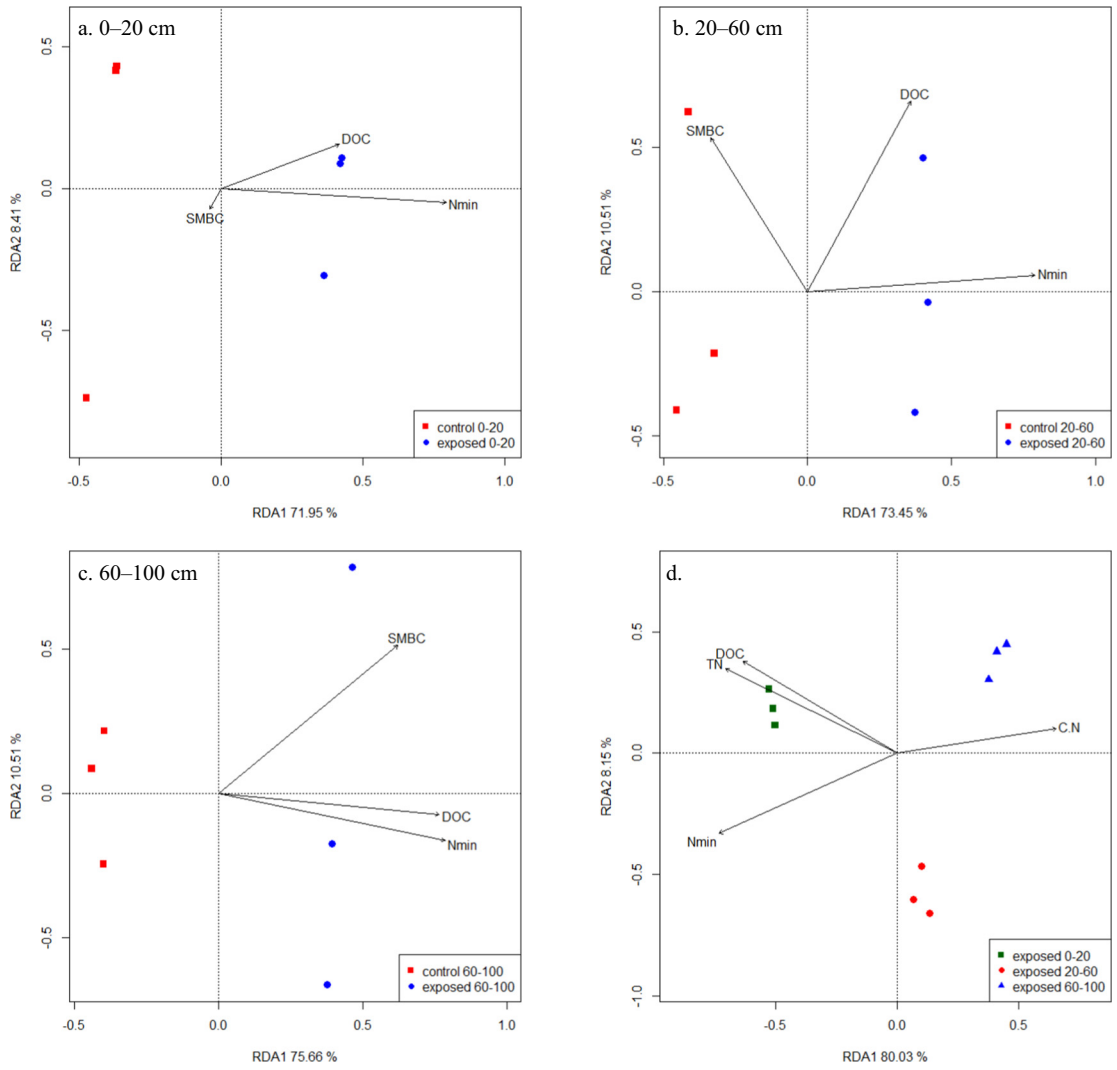

Fig. 5. Ordination plots of the results from the redundancy analysis (RDA) to identify relationships between bacterial OTUs and soil variables (black arrows) between the control and the exposed soils at 0–20 cm (a.), 20–60 cm (b.), 60–100 cm (c.) and that among depths of the exposed soil (d.) DOC and SMBC are short for the dissolved organic carbon and the microbial biomass carbon. N_{min} denote soil mineral nitrogen content. TN is short for the total notrogen content. C/N denote the soil carbon: nitrogen ratio.

both *r*-strategists and *K*-strategists were stimulated by subsoil exposure, with the former dominant at 20–60 cm, and the latter dominant at 60–100 cm.

Subsoil exposure was also accompanied by changes in the activity of enzymes involved in catalyzing the decomposition of organic carbon. At 20–60 cm, the activities of both BX and CB were stimulated (Table 1), promoting the decomposition of cellulose in plant residues and root exudates. At a depth of the 60–100 cm, the alteration of keystone groups (Tables 3, S4) and increased BX and BG activities (Table 4) suggested increased decomposition and mineralization of native recalcitrant C, such as aromatic compounds, polyphenols, chitin, and lignocellulose. These results agree well with previous findings (Chen et al., 2014), which reported that soil mineral N accelerated the decomposition of plant residues, whereas addition of DOC with N significantly accelerated the mineralization of native SOC. Decreased CB activities at 60–100 cm in the exposed soil compared with the control soil was possibly due to the spatial separation of the microorganisms from the plant residues and root exudates.

4.3. K_c and Q_{10} were consistently lower in exposed subsoil vs. topsoil

In exposed soil, a lower SOC decomposition rate in the subsurface soils was a joint result of C, N substrate limitation, reduced microbial biomass, lower enzyme activities and diversity of the microorganisms relative to the surface soil (Tables 1, S4, S5). The lower Q_{10} values in the exposed subsoil vs. topsoil could be largely attributable to the decreased TN, reduced microbial growth, and lower BX activities of the microorganisms in the subsoil (Tables 1, S4, S5). In the exposed soil, the predominant bacterial communities changed from *r*-strategists (Alphaproteobacteria) at 0–20 cm to *K*-strategists (Thermoleophilia) at 20–60 and 60–100 cm (Tables 3, S4; Fig. 4), which may have inherently varying Q_{10} patterns (Sun et al., 2018). Positive correlations of the copiotrophic groups (Alphaproteobacteria and unidentified_Actinobacteria) with K_c and Q_{10} values (Table S5) were probably due to their preference for labile C (Table S4) (Bai et al., 2017). In contrast, the oligotrophic niche could not provide sufficient energy for the activities of subsoil microorganisms, which would further attenuate Q_{10}. K_c was positively correlated with all of the enzyme activities, while Q_{10} was only correlated with BX activities (Table S5), suggesting that both slow and active pool might contribute to carbon loss, while the active pool was probably more susceptible to temperature changes. This situation potentially explained the similar Q_{10} values of the exposed soil from 20–60 and 60–100 cm, regardless of the divergent substrate utilization by microbes.

Such a reduction in Q_{10} in the exposed subsoil vs. topsoil has been rarely reported and contrasted with the higher Q_{10} values in the subsoil vs. the topsoil layers observed during incubation (Yan et al., 2017) and

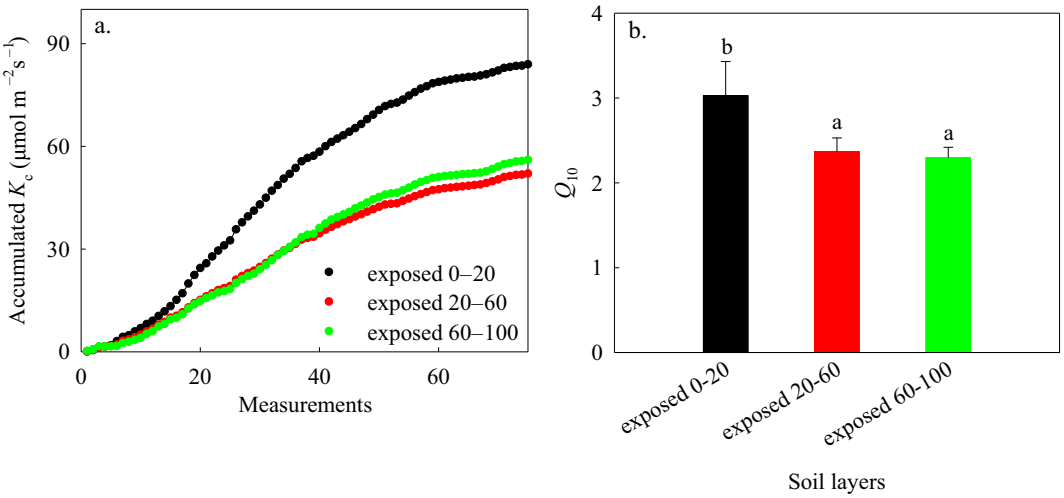

Fig. 6. The accumulated microbial SOC mineralization rates (K_c) with measurement numbers (a.) and mean Q_{10} values (b.) in the exposed soil over the study period.

in situ topsoil removal experiments (Gao et al., 2020). These studies found significantly higher SOC levels than our study, even in the subsoil. Soil carbon temperature sensitivity usually increases with increasing stability, which is regulated by chemical recalcitrance when the substrate availability is not limiting (Bosatta and Ågren, 1999). However, when the substrate availability is limited, the stability of substrates may be controlled by their physicochemical protection (Moinet et al., 2020), which is greater in subsoil than in topsoil, as subsoil stores more organic carbon in microaggregates while topsoil stor more organic carbon in microaggregates (Qin et al., 2019). These results suggest that SOC levels must be taken into account when estimating the potential effects of subsoil exposure on C loss under future climate change scenarios.

4.4. Extrapolated K_c and Q_{10} from the exposed soil to the control soil

In the exposed soil, the consistently lower K_c and Q_{10} at 20–60 and 60–100 cm than at 0–20 cm clearly illustrated the direction and magnitude of the responses of soil CO_2 emissions from subsoil exposure under future climate patterns. However, a drawback of the present study is the lack of determination of the SOC decomposition rate in the in situ control soil. It is plausible that previously buried soil at 20–60 cm and 60–100 cm was severely C and N-limited. Upon exposure to air, increased degradability of SOC would be expected, as spatial separation is assumed to be the main limiting factor for the decomposition of SOC buried in subsoils (Berhe, 2012). The disturbance of subsoil exposure exposes bacteria to air without the protection of aggregates, and increases the probability of microorganisms encountering and accessing degradable substrates, thus resulting in greater microbial C accessibility (Fierer et al., 2003). This process results in breakdown of aggregates, and exposes hitherto encapsulated SOC to microbial processes, exacerbating its vulnerability to decomposition (Lal, 2019). The input of C and N from subsoil exposure would relieve the energy limitation of the subsoils, enhance the mineralization of soil organic matter, and reduce the Q_{10}. The control soil would therefore be characterized by lower K_c and higher Q_{10} relative to the corresponding exposed soil. According to the similar K_c and Q_{10} values at 20–60 cm and 60–100 cm, it can be further deduced that the original Q_{10} of the control soil could be higher at 60–100 cm than at 20–60 cm.

Our results, especially the extrapolation, should be interpreted with caution, considering the complex Q_{10} patterns of various components under different conditions. However, this study provides a small step towards elaborating soil C cycling of the exposed subsoils in the eroded area, which may provide material for discussion. Future research should compare the SOC decomposition rate as well as its temperature sensitivity between the in situ and the exposed soils, so as to accurately access the response of carbon dynamics in the exposed subsoil to climate change.

5. Conclusions

Through a one-year incubation experiment using loessial soil on the Loess Plateau, our results revealed depth-specific responses of bacterial properties to subsoil exposure, which was strengthened by the poor C and N substrate availability. The exposed soil tended to have more abundant copiotrophic and aerobic Alphaproteobacteria and Actinobacteria, since more labile C and N substrates were released. In contrast, the oligotrophic and anaerobic Nitrospira and unidentified_Thermotogae were less abundant in the exposed soil than in the control soil. Especially at depths of 60–100 cm, bacterial community composition altered. Enzyme patterns revealed that soil mineral N (and DOC) stimulated the decomposition of exogenous organic C at 20–60 cm, and addition of DOC with N promoted the decomposition and mineralization of endogenous organic C at 60–100 cm, in the exposed vs. control soil, counteracting the energy limitation. The consistently lower K_c and Q_{10} in the exposed subsoil compared with the topsoil was a result of high protection of SOC by microaggregates, more severe substrate limitation, and the resulting altered bacterial community composition, as well reduced BX activity in the subsoil. This observation indicates that even when exposed to surface conditions, the positive response of SOC decomposition to climate warming can be limited, casting a new light on our current understanding of the role of subsoil exposure in the soil C budget of the eroded area. This study highlights the effects of anthropogenic soil redistribution and the potential to improve our projections of potential C loss in eroded areas under future climate change scenarios.

CRediT authorship contribution statement

Qiqi Sun: Formal analysis, Investigation, Writing – original draft, Visualization. **Shengli Guo:** Conceptualization, Methodology, Resources, Funding acquisition. **Rui Wang:** Investigation, Writing – review & editing, Project administration. **Jinming Song:** Data curation, Validation, Supervision.

Declaration of competing interest

The authors declare that they have no known competing financial interests or personal relationships that could have appeared to influence the work reported in this paper.

Acknowledgements

All authors hereby state that there is no conflict of interest to declare. This work is supported by Natural Science Foundation of China (No. 41371279, No. 41301322), China Postdoctoral Science Foundation (2018M643755), and Chinese Universities Scientific Fund (2014YB055). We would like to thank Editage (www.editage.cn) for English language editing.

Appendix A. Supplementary data

Supplementary data to this article can be found online at https://doi.org/10.1016/j.scitotenv.2020.144146.

References

Aylagas, E., Borja, Á., Tangherlini, M., Dell'Anno, A., Corinaldesi, C., Michell, C.T., et al., 2016. A bacterial community-based index to assess the ecological status of estuarine and coastal environments. Mar. Pollut. Bull. 114, 679–688.

Azam, F., Malfatti, F., 2007. Microbial structuring of marine ecosystems. Nat. Rev. Microbiol. 5, 782–791.

Bai, Z., Xie, H., Kao-Kniffin, J., Chen, B., Shao, P., Liang, C., 2017. Shifts in microbial trophic strategy explain different temperature sensitivity of CO2 flux under constant and diurnally varying temperature regimes. FEMS Microbiol. Ecol. 93, 1–12.

Bai, T., Tao, J., Li, Z., Shu, M., Yan, X., Wang, P., et al., 2019. Different microbial responses in top- and sub-soils to elevated temperature and substrate addition in a semiarid grassland on the Loess Plateau. Eur. J. Soil Sci. 70, 1025–1036.

Bardgett, R.D., Freeman, C., Ostle, N.J., 2008. Microbial contributions to climate change through carbon cycle feedbacks. ISME J. 2, 805–814.

Berhe, A.A., 2012. Decomposition of organic substrates at eroding vs. depositional landform positions. Plant Soil 350, 261–280.

Berhe, A.A., Harte, J., Harden, J.W., Torn, M.S., 2007a. The significance of the erosion-induced terrestrial carbon sink. Bioscience 57, 337–346.

Berhe, A.A., Torn, M.S., Harden, J.W., Harte, J., 2007b. Soil Erosion and Terrestrial Carbon Sequestration. Nri Research Highlights. No.9. USDA.

Bosatta, E., Ågren, G.I., 1999. Soil organic matter quality interpreted thermodynamically. Soil Biol. Biochem. 31, 1889–1891.

Brye, K.R., Slaton, N.A., Mozaffari, M., Savin, M.C., Norman, R.J., Miller, D.M., 2004. Short-term effects of land leveling on soil chemical properties and their relationships with microbial biomass. Soil Sci. Soc. Am. J. 68, 924–934.

Caporaso JG, Gordon JI. Global patterns of 16s rrna diversity at a depth of millions of sequences per sample. Proceedings of the National Academy of Sciences of the United States of America 2011; 108 Suppl 1: 4516.

Chen, R., Senbayram, M., Blagodatsky, S., Myachina, O., Dittert, K., Lin, X., et al., 2014. Soil C and N availability determine the priming effect: microbial N mining and stoichiometric decomposition theories. Glob. Chang. Biol. 20, 2356–2367.

Davidson, E.A., Belk, E., Boone, R.D., 1998. Soil water content and temperature as independent or confounded factors controlling soil respiration in a temperate mixed hardwood forest. Glob. Chang. Biol. 4, 217–227.

Davidson, E.A., Janssens, I.A., Luo, Y., 2006. On the variability of respiration in terrestrial ecosystems: moving beyond Q 10. Glob. Chang. Biol. 12, 154–164.

de Carvalho, T.S., Jesus, EdC, Barlow, J., Gardner, T.A., Soares, I.C., Tiedje, J.M., et al., 2016. Land use intensification in the humid tropics increased both alpha and beta diversity of soil bacteria. Ecology 97, 2760–2771.

Deforest, J.L., 2009. The influence of time, storage temperature, and substrate age on potential soil enzyme activity in acidic forest soils using MUB-linked substrates and l-DOPA. Soil Biol. Biochem. 41, 1180–1186.

Du, P.L., Rose, S.H., van Zyl, W.H., 2010. Exploring improved endoglucanase expression in Saccharomyces cerevisiae strains. Appl. Microbiol. Biotechnol. 86, 1503–1511.

Eck, H.V., 1987. Characteristics of exposed subsoil—at exposure and 23 years later. Agron. J. 79.

Edgar, R.C., 2013. UPARSE: highly accurate OTU sequences from microbial amplicon reads. Nat. Methods 10, 996.

Fang, C.M., Smith, P., Moncrieff, J.B., Smith, J.U., 2005. Similar response of labile and resistant soil organic matter pools to changes in temperature. Nature 433 (7021), 57–59.

Fernández-Escobar, R., Marin, L., Sánchez-Zamora, M.A., García-Novelo, J.M., Molina-Soria, C., Parra, M.A., 2009. Long-term effects of N fertilization on cropping and growth of olive trees and on N accumulation in soil profile. Eur. J. Agron. 31, 223–232.

Fierer, N., Schimel, J.P., Holden, P.A., 2003. Variations in microbial community composition through two soil depth profiles. Soil Biol. Biochem. 35, 167–176.

Fierer, N., Bradford, M.A., Jackson, R.B., 2008. Toward an ecological classification of soil bacteria. Ecology 88, 1354–1364.

Frock, A.D., Notey, rs, Kelly, rm, 2010. The genus Thermotoga: recent developments. Environ. Technol. 31, 1169–1181.

Fujii, K., Hartono, A., Funakawa, S., Uemura, M., Kosaki, T., 2011. Fluxes of dissolved organic carbon in three tropical secondary forests developed on serpentine and mudstone. Geoderma 163, 119–126.

Gao, X., Li, W., Salman, A., Wang, R., Du, L., Yao, L., et al., 2020. Impact of topsoil removal on soil CO2 emission and temperature sensitivity in Chinese Loess Plateau. Sci. Total Environ. 708, 135102.

Hu, D., Zang, Y., Mao, Y., Gao, B., 2019. Identification of molecular markers that are specific to the class Thermoleophilia. Front. Microbiol. 10.

Huang, M., Shao, M., Zhang, L., Li, Y., 2003. Water use efficiency and sustainability of different long-term crop rotation systems in the Loess Plateau of China. Soil Tillage Res. 72, 95–104.

Iqbal, J., Hu, R., Lin, S., Hatano, R., Feng, M., Lu, L., et al., 2009. CO2 emission in a subtropical red paddy soil (Ultisol) as affected by straw and N-fertilizer applications: a case study in Southern China. Agric. Ecosyst. Environ. 131, 292–302.

Jousset, A., Schulz, W., Scheu, S., Eisenhauer, N., 2011. Intraspecific genotypic richness and relatedness predict the invasibility of microbial communities. ISME J. 5, 1108.

Kirschbaum, M.U.F., 2013. Seasonal variations in the availability of labile substrate confound the temperature dependence of organic matter decomposition. Soil Biol. Biochem. 57, 568–576.

Lal, R., 2003. Soil erosion and the global carbon budget. Environ. Int. 29, 437–450.

Lal, R., 2019. Accelerated soil erosion as a source of atmospheric CO2. Soil Tillage Res. 188, 35–40.

Li, Y., Su, S., 1991. Comprehensive Study of Efficient and Ecological Economic System in Wangdonggou of Changwu County: Science and Technology Document Press.

Li, J., Yan, D., Pendall, E., Pei, J., Noh, N.J., He, J.-S., et al., 2018. Depth dependence of soil carbon temperature sensitivity across Tibetan permafrost regions. Soil Biol. Biochem. 126, 82–90.

Li, X., Wang, H.H., Li, X., Li, X.Y., Zhang, H.W., 2019. Shifts in bacterial community composition increase with depth in three soil types from paddy fields in China. Pedobiologia 77, 9.

Louca, S., Parfrey, L.W., Doebeli, M., 2016. Decoupling function and taxonomy in the global ocean microbiome. Science 353, 1272.

Marin-Spiotta, E., Chaopricha, N.T., Plante, A.F., Diefendorf, A.F., Mueller, C.W., Grandy, A.S., et al., 2014. Long-term stabilization of deep soil carbon by fire and burial during early Holocene climate change. Nat. Geosci. 7, 428–432.

Moinet, G.Y.K., Moinet, M., Hunt, J.E., Rumpel, C., Chabbi, A., Millard, P., 2020. Temperature sensitivity of decomposition decreases with increasing soil organic matter stability. Sci. Total Environ. 704.

Qin S, Chen L, Fang K, Zhang Q, Wang J, Liu F, et al. Temperature sensitivity of SOM decomposition governed by aggregate protection and microbial communities. Science Advances 2019; 5: eaau1218.

Shi, M., Li, J., Zhou, Q., Wang, G., Zhang, W., Zhang, Z., et al., 2020. Interactions between elevated CO2 levels and floating aquatic plants on the alteration of bacterial function in carbon assimilation and decomposition in eutrophic waters. Water Res. 171.

Simonin, M., Voss, K.A., Hassett, B.A., Rocca, J.D., Wang, S.-Y., Bier, R.L., et al., 2019. In search of microbial indicator taxa: shifts in stream bacterial communities along an urbanization gradient. Environ. Microbiol. 21, 3653–3668.

Sparks, D.L., Page, A.L., Helmke, P.A., Loeppert, R.H., Soltanpour, P.N., Tabatabai, M.A., et al., 1996. Methods of Soil Analysis. Part III. Chemical Methods.

Stallard, R.F., 1998. Terrestrial sedimentation and the carbon cycle: coupling weathering and erosion to carbon burial. Glob. Biogeochem. Cycles 12, 231–257.

Sun, Q., Hu, Y., Wang, R., Guo, S., Yao, L., Duan, P., 2018. Spatial distribution of microbial community composition along a steep slope plot of the Loess Plateau. Appl. Soil Ecol. 130, 226–236.

Sushko, S., Ananyeva, N., Ivashchenko, K., Vasenev, V., Kudeyarov, V., 2019. Soil CO_2 emission, microbial biomass, and microbial respiration of woody and grassy areas in Moscow (Russia). Journal of Soil & Sediments 19, 3217–3225.

Takriti, M., Wild, B., Schnecker, J., Mooshammer, M., Knoltsch, A., Lashchinskiy, N., et al., 2018. Soil organic matter quality exerts a stronger control than stoichiometry on microbial substrate use efficiency along a latitudinal transect. Soil Biol. Biochem. 121, 212–220.

Team RC. R: A Language and Environment for Statistical Computing. R Foundation for Statistical Computing, Vienna, Austria. http://www.R-project.org 2013.

Treude, N., Rosencrantz, D., Liesack, W., Schnell, S., 2003. Strain FAc12, a dissimilatory iron-reducing member of the Anaeromyxobacter subgroup of Myxococcales. FEMS Microbiol. Ecol. 44, 261–269.

Vance, E.D., Brookes, P.C., Jenkinson, D.S., 1987. An extraction method for measuring soil microbial biomass C. Soil Biol. Biochem. 19, 703–707.

Walling DE. The Impact of Global Change on Erosion and Sediment Transport by Rivers: Current Progress and Future Challenges. Fems Microbiology Ecology 2009; UNESCO: France.

Wang, Q., Garrity, G.M., Tiedje, J.M., Cole, J.R., 2007. Naïve Bayesian classifier for rapid assignment of rRNA sequences into the new bacterial taxonomy. Applied & Environmental Microbiology 73, 5261–5267.

Wang, R., Sun, Q., Wang, Y., Zheng, W., Yao, L., Hu, Y., et al., 2017. Contrasting responses of soil respiration and temperature sensitivity to land use types: cropland vs. apple orchard on the Chinese Loess Plateau. Sci. Total Environ. 621, 425–433.

Wang, M., Tian, Q., Liao, C., Zhao, R., Wang, D., Wu, Y., et al., 2019. The fate of litter-derived dissolved organic carbon in forest soils: results from an incubation experiment. Biogeochemistry 144, 133–147.

Weige, N., Shanchao, Y., Shiqing, L., Haizhou, H., Yufang, S., 2016. The factors related to carbon dioxide effluxes and production in the soil profiles of rain-fed maize fields. Agric. Ecosyst. Environ. 216, 177–187.

Xu, M., Qi, Y., 2001. Spatial and seasonal variations of Q10 determined by soil respiration measurements at a Sierra Nevadan Forest. Glob. Biogeochem. Cycles 15, 687–696.

Yan, D., Li, J., Pei, J., Cui, J., Nie, M., Fang, C., 2017. The temperature sensitivity of soil organic carbon decomposition is greater in subsoil than in topsoil during laboratory incubation. Sci. Rep. 7.

Yan, H., Yang, F., Gao, J., Peng, Z., Chen, W., 2019a. Subsoil microbial community responses to air exposure and legume growth depend on soil properties across different depths. Sentific Reports 9, 18536.

Yan, H.M., Yang, F., Gao, J.M., Peng, Z.H., Chen, W.M., 2019b. Subsoil microbial community responses to air exposure and legume growth depend on soil properties across different depths. Sci. Rep. 9, 11.

Zhi, L.I., Zheng, F.L., Liu, W.Z., 2010. Analyzing the spatial-temporal changes of extreme precipitation events in the Loess Plateau from 1961 to 2007. Journal of Natural Resources 25, 291–299.